Mathematical Biosciences and Engineering

http://www.aimspress.com/journal/mbe

MBE, 19(6): 6396–6414.
DOI: 10.3934/mbe.2022300
Received: 05 March 2022
Revised: 11 April 2022
Accepted: 15 April 2022
Published: 24 April 2022

Research article

Transmission dynamics of brucellosis with patch model: Shanxi and Hebei Provinces as cases

Yaoyao Qin, Xin Pei*, Mingtao Li and Yuzhen Chai

School of Mathematics, Taiyuan University of Technology, Taiyuan 030024, China

* **Correspondence:** Email: peixin1120@126.com.

Abstract: Brucellosis is a zoonotic disease caused by Brucella, and it is an important infectious disease all over the world. The prevalence of brucellosis in the Chinese mainland has some spatial characteristics besides the temporal trend in recent years. Due to the large-scale breeding of sheep and the frequent transportation of sheep in various regions, brucellosis spreads wantonly in pastoral areas, and human brucellosis spreads from traditional pastoral areas and semi-pastoral areas in the north to non-pastoral areas with low incidence in the south. In order to study the influence of sheep immigration on the epidemic transmission, a patch dynamics model was established. In each patch, the sub-model was composed of humans, sheep and Brucella. The basic reproduction number, disease-free equilibrium and positive equilibrium of the model were discussed. On the other hand, taking Shanxi Province and Hebei Province as examples, we carried out numerical simulations. The results show that the basic reproduction numbers of Shanxi Province and Hebei Province are 0.7497 and 0.5022, respectively, which indicates that the current brucellosis in the two regions has been effectively controlled. To reduce brucellosis faster in the two provinces, there should be a certain degree of sheep immigration from high-infection area to low-infection areas, and reduce the immigration of sheep from low-infection areas to high-infection areas.

Keywords: brucellosis; sheep immigration; patch model; basic reproduction number

1. Introduction

Brucellosis is one of the common zoonotic diseases, and it mainly infects livestock and has been reported in various countries [1]. The main reason people suffer from brucellosis is eating food contaminated with Brucella or contacting the secretions and excreta of sick animals; people don't infect each other [2]. There are many kinds of Brucella, including Brucella of cattle, sheep, pigs, dogs and mice, of which the main infectious sources are sick sheep and cattle [3, 4]. With the large-scale management of the sheep industry and the frequent trading of sheep products among regions, the

liquidity of sick sheep has increased. In the past 30 years, brucellosis epidemic areas have gradually shifted from pastoral areas (i.e., Inner Mongolia, Xinjiang, Tibet, Qinghai and Ningxia) to grassland and agricultural areas (i.e., Shanxi, Liaoning, Hebei, Shandong and Jilin). Especially since 2004, the affected areas have expanded from the north to the south of China [5, 6]. There is evidence that the epidemic of brucellosis in the south is caused by infected animals imported from other regions [7]. Therefore, the development of animal husbandry and the immigration of sheep are the most commonly accepted explanations for the prevalence of human brucellosis.

Mathematical modeling is a good tool to study diseases and give measures for disease control. For example, mathematical models have played a key role in predicting and controlling the disease for the novel coronavirus currently present globally, Ma et al. [8] studied the effect of mask use on controlling the spread of COVID-19 by constructing a model, and Asamoah et al. [9] studied the optimal control and cost effectiveness of COVID-19 through modeling. Some mathematical models have been used in the study of brucellosis. For example, Li et al. [2] studied the transmission mechanism of brucellosis in the Hinggan League of Inner Mongolia, and the results showed that banning the mixed feeding of basic ewes and other sheep, vaccination, detection and culling were the effective strategies. Hou and Sun [10] established a multi-stage dynamic model of sheep brucellosis transmission, and it was concluded that the birth rate, vaccination rate and culling rate of sheep play an important role in the transmission of brucellosis. From the investigation and comparison of the effects of vaccination and culling strategies, the latter is better than the former. Chen et al. [11] studied the spatial distribution of human brucellosis in Shanxi Province and found that the proportion of affected cities and towns increased from 31.5% in 2005 to 82.5% in 2014. These papers only studied the temporal and spatial characteristics of human brucellosis and established a dynamic model according to the pathogenesis and propagative law of brucellosis in different epidemic areas. The immigration of sheep among patches is an important factor causing the spread of brucellosis, but there is little work.

With regard to the research on the spatial transmission of brucellosis, Zhang et al. [12] established a multi-patch dynamic model of cattle brucellosis, and they obtained that the dispersal of susceptible populations of each patch and the centralization of infected cattle to patches with large breeding scale are conducive to the control of the disease. However, the basic reproduction number, the uniqueness of the positive equilibrium and the global asymptotic stability have not been further analyzed, and there is no numerical simulation of practical problems. Sick sheep are a major source of human brucellosis. Based on the above research, this paper established a patch model composed of people, sheep and Brucella. The transmission of sheep brucellosis among patches was analyzed qualitatively and quantitatively, and the prevention and control measures were put forward in combination with practical problems.

The article is organized as follows. In Section 2, an n-patch dynamics model was proposed. In Section 3, we gave the mathematical analysis of the model, including the basic reproduction number, disease-free equilibrium and positive equilibrium. In Section 4, taking two patches in Shanxi Province and Hebei Province as examples, the numerical simulation was given. In Section 5, a brief conclusion was made.

2. Model formulation

The spatial distribution of human brucellosis shows that there is inter-provincial transmission of human brucellosis in China. Therefore, we regarded each province as an isolated patch. Assuming there are n patches, a multi-patch model composed of humans, sheep and Brucella was established. We made some assumptions about the model: that human brucellosis is mainly transmitted by sick sheep, and that environmental brucellosis also causes infection in susceptible people and sheep. There are few reports of human-to-human transmission of brucellosis, so human-to-human and human-to-animal transmission are ignored. Since sheep are the main source of infection, we considered only sheep immigration among patches and not human immigration among patches. In patch i, the population is divided into three classes: S_i^h, I_i^h and Y_i^h, which are susceptible, acute and chronic brucellosis patients at time t, respectively. Sheep are divided into two classes: S_i and I_i , which are the number of susceptible sheep and infected sheep at time t, respectively. During infection, the infected sheep release brucella into the environment, and the number of brucella in the environment is denoted by W_i. The flow chart of brucellosis is shown in Figure 1.

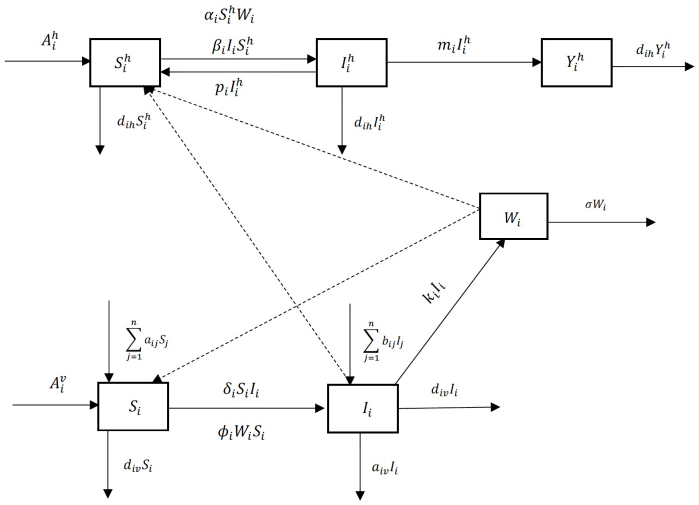

Figure 1. Flow chart of brucellosis transmission among patches.

Based on the model flow chart, we established a multi-patch dynamics model including sheep, humans and bacteria in the environment:

$$\begin{cases} \frac{dS_i^h}{dt} = A_i^h - d_{ih}S_i^h - \beta_i S_i^h I_i - \alpha_i S_i^h W_i + p_i I_i^h, \\ \frac{dI_i^h}{dt} = \beta_i S_i^h I_i + \alpha_i S_i^h W_i - d_{ih} I_i^h - p_i I_i^h - m_i I_i^h, \\ \frac{dY_i^h}{dt} = m_i I_i^h - d_{ih} Y_i^h, \\ \frac{dS_i}{dt} = A_i^v - d_{iv} S_i - \delta_i S_i I_i - \phi_i W_i S_i + \sum_{j=1}^{n} a_{ij} S_j, \\ \frac{dI_i}{dt} = \delta_i S_i I_i + \phi_i W_i S_i - d_{iv} I_i - a_{iv} I_i + \sum_{j=1}^{n} b_{ij} I_j, \\ \frac{dW_i}{dt} = k_i I_i - \sigma W_i, \\ i = 1, 2..., n, \end{cases} \tag{2.1}$$

where A_i^h and d_{ih} are the numbers of birth and natural mortality of people per unit time, respectively; A_i^v and d_{iv} are the birth number and sale rate of sheep per unit time, respectively; p_i is the transfer rate

from acute infections to susceptible individuals; m_i is the transfer rate from acute infections to chronic infections; α_i is the transmission rate of Brucella to susceptible humans; β_i is the transmission rate of infectious sheep to susceptible humans; δ_i is the transmission rate of infectious sheep to susceptible sheep; ϕ_i is the transmission rate of Brucella to susceptible sheep; a_{iv} is the disease-related culling rate of infectious sheep; a_{ij} and b_{ij} are the immigration rates of the susceptible sheep and infectious sheep from the jth patch to the ith patch for $i \neq j$; $-a_{ii} = \sum_{i\neq j} a_{ji}$ and $-b_{ii} = \sum_{i\neq j} b_{ji}$ are the emigration rates of the susceptible sheep and infectious sheep; k_i is the amount of Brucella released from infected sheep; and σ is the decay rate of Brucella.

Since the last three equations of system (2.1) are independent of the first three equations, we only studied the following system for the dynamic analysis of (2.1):

$$\begin{cases} \frac{dS_i}{dt} = A_i^v - d_{iv}S_i - \delta_i S_i I_i - \phi_i W_i S_i + \sum_{j=1}^{n} a_{ij}S_j, \\ \frac{dI_i}{dt} = \delta_i S_i I_i + \phi_i W_i S_i - d_{iv}I_i - a_{iv}I_i + \sum_{j=1}^{n} b_{ij}I_j, \\ \frac{dW_i}{dt} = k_i I_i - \sigma W_i, \\ i = 1, 2..., n. \end{cases} \tag{2.2}$$

3. Dynamic analysis of model

Firstly, we considered the existence and uniqueness of the disease-free equilibrium of (2.2).

Let $E^0 = (S_1^0, S_2^0, ..., S_n^0, 0, ..., 0, 0, ..., 0)$ be the disease-free equilibrium of (2.2); then $S^0 = (S_1^0, S_2^0, ..., S_n^0)$ is the positive equilibrium of the following subsystem:

$$\frac{dS_i}{dt} = A_i^v - d_{iv}S_i + \sum_{j=1}^{n} a_{ij}S_j, \qquad i = 1, 2, ..., n. \tag{3.1}$$

According to $A_i^v - d_{iv}S_i + \sum_{j=1}^{n} a_{ij}S_j = 0$, we define an auxiliary matrix

$$M_1 = \begin{bmatrix} d_{1v} - a_{11} & -a_{12} & \dots & -a_{1n} \\ -a_{21} & d_{2v} - a_{22} & \dots & -a_{2n} \\ \vdots & \vdots & \ddots & \vdots \\ -a_{n1} & -a_{n2} & \dots & d_{nv} - a_{nn} \end{bmatrix}_{n\times n}.$$

Then, $M_1 S = A^v$, where $S = (S_1, S_2, ..., S_n)^T, A^v = (A_1^v, A_2^v, .., A_n^v)^T$. Note that M_1 is an irreducible M-matrix (Appendix A [13]), and $M_1 S = A^v$ has a unique solution S. According to corollary 4.3.2 [14], $M_1^{-1}$is a positive matrix; then, $S = M_1^{-1}A^v > 0$, so $S^0 = (S_1^0, S_2^0, ..., S_n^0)$ is the only positive equilibrium of (3.1).

Define $s(M)$ as the spectral bound of matrix M.

$s(M)$=max{Reλ:λ is an eigenvalue of M}.

$M_1 S = A^v$, so $-M_1 S = -A^v$. Since $-M_1$ is an irreducible Metzler matrix , by the Perron-Frobenius Theorem [15], $s(-M_1)$ is a zero solution of the characteristic polynomial, there is no other eigenvalue λ so that $R(\lambda) = s(-M_1)$, and there is only one positive eigenvector for the eigenvalue $s(-M_1)$. Let $V = (v_1, v_2, \dots, v_n)$ be a positive eigenvector associated with $s(-M_1)$; then, $-M_1 V = s(-M_1)V =$

$-A^v$, so $s(-M_1) < 0$, and hence all eigenvalues of $-M_1$ have negative real parts. Since (3.1) is a linear system, $S^0 = (S_1^0, S_2^0, \ldots, S_n^0)$ is globally asymptotically stable on $S \in R_+^n \setminus 0$. Thus, $E^0 = (S_1^0, S_2^0, ..., S_n^0, 0, 0, ..., 0, 0, 0, ..., 0)$ is the disease-free equilibrium of (2.2).

3.1. Basic reproduction number

To derive the basic reproduction number R_0 for (2.2), we ordered the infected variables first by disease state, then by patch, i.e.,

$$I_1, I_2, ..., I_n, W_1, W_2, ..., W_n.$$

Applying the method of the next generation matrix [13], we can obtain the expression of the basic reproduction number; define

$$\mathcal{F} = \begin{bmatrix} \delta_1 S_1 I_1 + \phi_1 W_1 S_1 \\ \vdots \\ \delta_n S_n I_n + \phi_n W_n S_n \\ 0 \\ \vdots \\ 0 \end{bmatrix}, \qquad \mathcal{V} = \begin{bmatrix} (d_{1v} + a_{1v})I_1 - \sum_{j=1}^n b_{1j} I_j \\ \vdots \\ (d_{nv} + a_{nv})I_n - \sum_{j=1}^n b_{nj} I_j \\ -k_1 I_1 + \sigma W_1 \\ \vdots \\ -k_n I_n + \sigma W_n \end{bmatrix}.$$

$F = \begin{bmatrix} F_1 & F_2 \\ 0 & 0 \end{bmatrix}$, $V = \begin{bmatrix} V_1 & 0 \\ V_3 & V_4 \end{bmatrix}$, where $F_1 = (\delta_{ij}(\delta_i S_i^0))_{n\times n}$, $F_2 = (\delta_{ij}(\phi_i S_i^0))_{n\times n}$, $V_1 = (\delta_{ij}(d_{iv} + a_{iv}) - B)_{n\times n}$, $B = (b_{ij})_{n\times n}$, $V_3 = (\delta_{ij}(-k_i))_{n\times n}$, $V_4 = (\delta_{ij}(\sigma))_{n\times n}$.

δ_{ij} denotes the Kronecker delta (i.e., 1 when i = j and 0 otherwise). Define $M = F - V$.

$$V^{-1} = \begin{bmatrix} V_1^{-1} & 0 \\ -V_4^{-1} V_3 V_1^{-1} & V_4^{-1} \end{bmatrix}, \qquad FV^{-1} = \begin{bmatrix} F_1 V_1^{-1} - F_2 V_4^{-1} V_3 V_1^{-1} & F_2 V_4^{-1} \\ 0 & 0 \end{bmatrix};$$

then, $R_0 = \rho(FV^{-1}) = \rho(F_1 V_1^{-1} - F_2 V_4^{-1} V_3 V_1^{-1})$, where $\rho(FV^{-1})$ represents the spectral radius of the matrix FV^{-1}. In particular, the basic reproduction number of the single patch model (2.2) is $R_{0i} = \frac{\delta_i S_i^0 \sigma + k_i \phi_i S_i^0}{(d_{iv} + a_{iv})\sigma}$.

Corollary 3.1. $\min_{1\le i\le n} R_{0i} \le R_0 \le \max_{1\le i\le n} R_{0i}$.

Proof. Through the expression of R_0, we gained $F_1 V_1^{-1} - F_2 V_4^{-1} V_3 V_1^{-1} = (F_1 - F_2 V_4^{-1} V_3) V_1^{-1}$.

Let

$$H = F_1 - F_2 V_4^{-1} V_3 = \begin{bmatrix} \frac{\delta_1 S_1^0 \sigma + k_1 \phi_1 S_1^0}{\sigma} & 0 & \ldots & 0 \\ 0 & \frac{\delta_2 S_2^0 \sigma + k_2 \phi_2 S_2^0}{\sigma} & \ldots & 0 \\ \vdots & \vdots & \ddots & \vdots \\ 0 & 0 & \ldots & \frac{\delta_n S_n^0 \sigma + k_n \phi_n S_n^0}{\sigma} \end{bmatrix},$$

then, $R_0 = \rho(HV_1^{-1})$.

Since V_1 is the M-matrix, V_1^{-1} is a nonnegative matrix. We apply Fischer's inequality (Theorems 2.5.4(e) [16]) and 3.4 [17] to estimate the diagonal entries of matrix V_1^{-1}.

For example, let $V_1 = (a_{ij})_{n\times n}$ and $V_1^{-1} = (\alpha_{ij})_{n\times n}$; then, $\frac{1}{a_{ii}} \le \alpha_{ii}$, $i = 1, 2, ..., n$. Therefore, $0 \le diag\{\frac{1}{d_{1v}+a_{1v}}, ..., \frac{1}{d_{nv}+a_{nv}}\} \le diag\{\frac{1}{d_{1v}+a_{1v}-b_{11}}, ..., \frac{1}{d_{nv}+a_{nv}-b_{nn}}\} \le diag\{\alpha_{11}, ..., \alpha_{nn}\} \le V_1^{-1}$.

So, $\min_{1\le i\le n} R_{0i} \le R_0$.

Let $G = V_1 + B = diag\{d_{1v} + a_{1v}, ..., d_{nv} + a_{nv}\}$; then, $I(V_1G^{-1}) = I \Rightarrow I(GV_1^{-1}) = I$, where $I = (1, 1, ..., 1)_{1\times n}$, which implies that the spectral radius of GV_1^{-1} is 1, and hence $\rho(V_1^{-1}) = \rho(G^{-1}GV_1^{-1}) \le \rho(G^{-1})\rho(GV_1^{-1}) = \rho(G^{-1})$.

So, $\rho(HV_1^{-1}) \le \rho(H)\rho(V_1^{-1}) \le \rho(H)\rho(G^{-1}) \le \max_{1\le i\le n} R_{0i}$.

Based on the above, $\min_{1\le i\le n} R_{0i} \le R_0 \le \max_{1\le i\le n} R_{0i}$.

Lemma 3.1. *There hold two equivalences [13]:*

$$R_0 < 1 \Longleftrightarrow s(M) < 0, R_0 > 1 \Longleftrightarrow s(M) > 0.$$

By Theorem 2 [13], the disease-free equilibrium E^0 is locally asymptotically stable if $R_0 < 1$ and is unstable if $R_0 > 1$.

Next, we studied the global dynamics of (2.2), the disease-free equilibrium E^0 is globally attractive if $R_0 < 1$, and (2.2) has a positive equilibrium if $R_0 > 1$.

Lemma 3.2. *Let* $k = \max\{k_i : 1 \le i \le n\}, d_v = \min\{d_{iv} : 1 \le i \le n\}, N^* = \frac{A}{d_v}$, *where* $A = \sum_{i=1}^n A_i^v$. *Every forward orbit of* (2.2) *eventually enters into* $G = \{(S, I, W) \in R_+^{3n} : \sum_{i=1}^n (S_i + I_i) \le N^*, \sum_{i=1}^n W_i \le \frac{kN^*}{\sigma}\}$, *and G is positively invariant for* (2.2).

Theorem 3.1. *When* $R_0 < 1$, *the disease-free equilibrium of system* (2.2) *is globally asymptotically stable in G [12].*

Theorem 3.2. *When* $R_0 > 1$, *then* (2.2) *admits at least one positive equilibrium, and there is a positive constant* κ *such that every solution* $\phi_t(\chi_0) = (S(t), I(t), W(t))$ *of* (2.2) *with* $\chi_0 = (S_1(0), ..., S_n(0), I_1(0), ..., I_n(0), W_1(0), ..., W_n(0)) \in R_+^n \times R_+^n \setminus \{0\} \times R_+^n \setminus \{0\}$ *satisfies*

$$\lim_{t\mapsto\infty} I_i(t) > \kappa, \lim_{t\mapsto\infty} W_i(t) > \kappa, (i = 1, 2, ..., n). \tag{3.2}$$

Proof. Let

$X = \{(S_1, .., S_n, I_1, ..., I_n, W_1, ..., W_n) : S_i \ge 0, I_i \ge 0, W_i \ge 0, i = 1, 2, ..., n\}$.

$X_0 = \{(S_1, .., S_n, I_1, ..., I_n, W_1, ..., W_n) \in X : I_i > 0, W_i > 0, i = 1, 2, ..., n\}$.

$\partial X_0 = X \setminus X_0 = \{(S_1, .., S_n, I_1, ..., I_n, W_1, ..., W_n) \in X :$ for some $i \in \{1, 2, ..., n\}, I_i = 0, W_i = 0\}$.

Then, we showed that (2.2) is uniformly persistent with respect to $(X_0, \partial X_0)$.

Clearly, X and X_0 are positively invariant, and ∂X_0 is relatively closed in X. Furthermore, system (2.2) is point dissipative [18]. Set $M_\partial = \{(S(0), I(0), W(0)) : (S(t), I(t), W(t))$ satisfies (2.2) and $(S(t), I(t), W(t)) \in \partial X_0, \forall t \ge 0\}$.We next show that $M_\partial = \{(S, 0, 0) : S \ge 0\}$.

Set $(S(0), I(0), W(0)) \in M_\partial$; then, $I(t) = 0, W(t) = 0, \forall t \ge 0$. Suppose not, then there exist an $i_0, 1 \le i_0 \le n$, and a $t_0 \ge 0$ such that $I_{i0}(t_0) > 0$. Here we only analyzed $I(t)$, because the change of $W(t)$ depends on the change of $I(t)$. If $I_i(t) > 0$, then $W_i(t) > 0$; if $I_i(t) = 0$, then $W_i(t)$ eventually tends to 0.

We partition $\{1, 2, ..., n\}$ into two sets Q_1 and Q_2 such that

$I_i(t_0) = 0, \forall i \in Q_1$,

$I_i(t_0) > 0, \forall i \in Q_2$.

Defined by M_∂, Q_1 is a non-empty set. Since $I_{i0} > 0$, Q_2 is non-empty. For any $j \in Q_1$, we have $I_j'(t_0) = \delta_j S_j(t_0)I_j(t_0) + \phi_j W_j(t_0)S_j(t_0) - d_v I_j(t_0) - a_v I_j(t_0) + \sum_{i=1}^n b_{ji}I_i(t_0) = \phi_j W_j(t_0)S_j(t_0) + \sum_{i=1}^n b_{ji}I_i(t_0) \ge b_{ji_0}I_{i0}(t_0) > 0$.

Then exist an $\varepsilon_0 > 0$, when $t_0 < t < t_0 + \varepsilon_0$, there is $I_j(t) > 0, j \in Q_1$, we can restrict $\varepsilon_0 > 0$ small enough such that $t_0 < t < t_0 + \varepsilon_0, I_i(t) > 0, i \in Q_2$. This shows that when $t_0 < t < t_0 + \varepsilon_0$, $(S(t), I(t), W(t)) \notin \partial X_0$, which contradicts $(S(0), I(0), W(0)) \in M_\partial$, so $M_\partial = \{(S, 0, 0) : S \geq 0\}$.

Obviously, M_∂ has only one equilibrium E^0. We chose $\eta > 0$ small enough such that $s(M - M_\eta) > 0$, where $M_\eta = \begin{bmatrix} A_\eta & B_\eta \\ 0 & 0 \end{bmatrix}$, $A_\eta = \delta_{ij}(\delta_i \eta)_{n\times n}$, $B_\eta = \delta_{ij}(\phi_i \eta)_{n\times n}$. Consider the perturbed system of (3.1)

$$S_i^{'} = A_i^v - (d_{iv} + \delta_i \varepsilon_1 + \phi_i \varepsilon_1) S_i + \sum_{j=1}^{n} a_{ij} S_j. \tag{3.3}$$

First, with regard to our previous analysis of the system (3.1), restrict $\varepsilon_1 > 0$ small enough so that the system (3.3) has a unique equilibrium point $S^*(\varepsilon_1)$ and is globally asymptotically stable, and $S^*(\varepsilon_1)$ is continuous in ε_1. Therefore, we can further restrict $\varepsilon_1 > 0$ small enough such that $S^*(\varepsilon_1) > S^0 - \eta$.

Let us consider an arbitrary positive solution $(S(t), I(t), W(t))$ of (2.2); then, $\lim\limits_{t\to\infty} \sup \max\limits_i \{I_i(t)\} > \varepsilon_1$. Suppose there is a $T > 0$ such that $I_i(t) \leq \varepsilon_1, i = 1, 2, ..., n$, for $t \geq T$; then for $t \geq T$, we have

$$S_i' \geq A_i^v - (d_{iv} + \delta_i \varepsilon_1 + \phi_i \varepsilon_1) S_i + \sum_{j=1}^{n} a_{ij} S_j, \quad i = 1, 2..., n. \tag{3.4}$$

Since the equilibrium $S^*(\varepsilon_1)$ of system (3.3) is globally asymptotically stable, and $S^*(\varepsilon_1) > S^0 - \eta$, there is $T_1 > 0$ such that $S(t) \geq S^0 - \eta$ for $t > T_1 + T$. Therefore, when $t > T_1 + T$,

$$I_i' \geq \delta_i (S_i^0 - \eta) I_i + \phi_i W_i (S_i^0 - \eta) - d_{iv} I_i - a_{iv} I_i + \sum_{j=1}^{n} b_{ij} I_j \quad i = 1, 2, ..., n.$$

Since the matrix $(M - M_\eta)$ has a positive eigenvalue $s(M - M_\eta)$ with a positive eigenvector, according to the comparison principle [19], $\lim\limits_{t\to\infty} I_i(t) = \infty$; then, $\lim\limits_{t\to\infty} W_i(t) = \infty, i = 1, 2, ..., n$, which leads to a contradiction.

For the system (3.1), we noted that S^0 is globally asymptotically stable. From the above, we can see that E^0 is an isolated invariant set in X, $W^s(E^0) \cap X_0 = \varnothing$. Clearly, each orbit in M_∂ converges to E^0, and E^0 is acyclic in M_∂. According to the theorem 4.6 [20], the system (2.2) is uniformly persistent with respect to $(X_0, \partial X_0)$. By the theorem 2.4 [21], (2.2) has an equilibrium $E^* = (S_1^*, ..., S_n^*, I_1^*, ..., I_n^*, W_1^*, ..., W_n^*) \in X_0, S^* \in R_+^n, I^* \in int(R_+^n), W^* \in int(R_+^n)$. Where $S^* \in R_+^n \setminus \{0\}$, supposed that $S^* = 0$, from the second equation of system (2.2), we can get $0 = -\sum_{i=1}^{n} (d_{iv} + a_{iv}) I_i^*$, since $d_{iv} + a_{iv} \neq 0$; then, $I_i^* = 0, i = 1, 2, ..., n$, a contradiction. Through the first equation of system (2.2) and the irreducibility of matrix $(a_{ij})_{n\times n}$, $S^* \in int(R_+^n), \forall t > 0$; then, (S^*, I^*, W^*) is the positive equilibrium of system (2.2).

3.2. Uniqueness and uniform persistence of endemic equilibrium

We restricted the system (2.2) by assuming that the disease-related culling rate is 0, and the immigration rate of susceptible sheep and infected sheep is the same, that is, $a_{ij} = b_{ij}, i = 1, 2, ..., n$;

then, the model of system (2.2) becomes

$$\begin{cases} \frac{dS_i}{dt} = A_i^v - d_{iv}S_i - \delta_i S_i I_i - \phi_i W_i S_i + \sum_{j=1}^n b_{ij} S_j, \\ \frac{dI_i}{dt} = \delta_i S_i I_i + \phi_i W_i S_i - d_{iv} I_i + \sum_{j=1}^n b_{ij} I_j, \\ \frac{dW_i}{dt} = k_i I_i - \sigma W_i, \\ i = 1, 2..., n. \end{cases} \tag{3.5}$$

Add the first two equations of the system (3.5):

$$\frac{dN_i}{dt} = A_i^v - d_{iv}N_i + \sum_{j=1}^{n} b_{ij}N_j, \qquad i = 1, 2, ..., n. \tag{3.6}$$

By the conclusion of system (3.1), system (3.6) has a unique positive equilibrium $N^* = (N_1^*, N_2^*, ..., N_n^*)$, and system (3.5) has the following limit system:

$$\begin{cases} \frac{dI_i}{dt} = \delta_i(N_i^* - I_i)I_i + \phi_i W_i(N_i^* - I_i) - d_{iv} I_i + \sum_{j=1}^n b_{ij} I_j, \\ \frac{dW_i}{dt} = k_i I_i - \sigma W_i, \\ i = 1, 2..., n. \end{cases} \tag{3.7}$$

Lemma 3.3. *For system* (3.7)*, the set* $G_1 = \{(I, W) \in R_+^{2n} : I_i \le N_i, W_i \le \frac{k_i N_i}{\sigma}, i = 1, 2, ..., n\}$ *is positively invariant.*

Theorem 3.3. *When* $R_0 > 1$*, the system* (3.7) *admits a unique endemic equilibrium* $\overline{E}^* = \{I_1^*, ..., I_n^*, W_1^*, ..., W_n^*\}$*, which is globally asymptotically stable with respect to* $(I(0), W(0)) \in G_1$.

Proof. Through the definition on the right side of the system (3.7), $F\colon G_1 \to G_1$. Obviously, F is continuously differentiable and is cooperative on G_1, and $DF(I, W)$ is irreducible for every $(I, W) \in G_1$. $F(0) = 0$, and $F_i(I, W) \ge 0$ for all $(I, W) \in G_1$ with $I_i = 0, W_i = 0, i = 1, 2, ..., n$.

For $\forall \alpha \in (0, 1)$ and $(I, W) = (I_1, ..., I_n, W_1, ..., W_n) \in G_1$, we have

$\alpha\delta_i(N_i^* - \alpha I_i)I_i + \alpha\phi_i W_i(N_i^* - \alpha I_i) - \alpha d_{iv} I_i + \alpha \sum_{j=1}^n b_{ij} I_j > \alpha[\delta_i(N_i^* - I_i)I_i + \phi_i W_i(N_i^* - I_i) - d_{iv} I_i + \sum_{j=1}^n b_{ij} I_j], i = 1, 2, ..., n.$

$k_i \alpha I_i - \sigma\alpha W_i = \alpha(k_i I_i - \sigma W_i), i = 1, 2, ..., n.$

Therefore, F is strictly sublinear on G_1 [22].

Let $s(DF(0)) = \overline{M} = \begin{bmatrix} F_1 - V_1 & F_2 \\ -V_3 & -V_4 \end{bmatrix}$, where $F_1 = (\delta_{ij}(\delta_i N_i^*))_{n\times n}$, $F_2 = (\delta_{ij}(\phi_i N_i^*))_{n\times n}$, $V_1 = (\delta_{ij}(d_{iv} - B)_{n\times n}$, $B = (b_{ij})_{n\times n}$, $V_3 = (\delta_{ij}(-k_i))_{n\times n}$, $V_4 = (\delta_{ij}(\sigma))_{n\times n}$. Then, $\overline{M}$ is an irreducible Metzler matrix. According to the Perron-Frobenius theorem, $s(\overline{M})$ is an eigenvalue with a positive eigenvector, and let its positive eigenvector be $x = (x_1, ..., x_n, x_{n+1}, ..., x_{2n})$, so $\overline{M}x = s(\overline{M})x = (\delta_1 x_1^2 + \phi_1 x_1 x_{n+1}, ..., \delta_n x_n^2 + \phi_n x_n x_{2n}, 0, ..., 0)^T$; then, $s(\overline{M}) > 0$. From lemma 3.1 and corollary 3.2 [22], the system (3.7) has a unique positive equilibrium $\overline{E}^* = \{I_1^*, ..., I_n^*, W_1^*, ..., W_n^*\}$.

Theorem 3.4. *When* $R_0 > 1$*, the system* (3.5) *has a unique endemic equilibrium* $E^* = (S_1^*, ..., S_n^*, I_1^*, ..., I_n^*, W_1^*, ..., W_n^*)$*, which is globally asymptotically stable with respect to* $(S(0), I(0), W(0)) \in G$.

Proof. Let $\psi(t)$ be the corresponding flow of system (3.7). According to the strong monotonicity of $\psi(t)$, $S_i^* = N_i^* - I_i^* > 0, i = 1, 2, ..., n$, so the system (3.5) has a unique positive equilibrium $E^* = (S_1^*, ..., S_n^*, I_1^*, ..., I_n^*, W_1^*, ..., W_n^*)$. Next, we prove the globally asymptotic stability of the positive equilibrium E^*.

Let $\phi(t)$: $R_+^{3n} \to R_+^{3n}$ be the solution semiflow of system (3.5), and let ω be the ω limit set of $\phi(S(0), I(0), W(0)) \in G$. By lemma 2.1′ [21], ω is an internal chain transitive set for $\phi(t)$. Clearly, when $R_0 > 1$, the system (3.5) has only two equilibria, E^0 and E^*, by $S^0 = (S_1^0, S_2^0, ..., S_n^0)$ is globally asymptotically stable on $R_+^n \backslash \{0\}$ and theorem 3.1, it is easy to know that $\phi(t)$ satisfies theorem 1.2.2 [23]. Thus, ω is E^0 or E^*. Next, we show that $\omega = \{E^*\}$.

Let's assume $\omega = \{E^0\}$; then, $\lim\limits_{t\to\infty} S_i(t) = S_i^0, \lim\limits_{t\to\infty} I_i(t) = 0, \lim\limits_{t\to\infty} W_i(t) = 0, (i = 1, 2, ..., n)$.

Since $s(M) > 0$, we can choose a small enough $\epsilon > 0$ so that $s(M - M_\epsilon) > 0$, where $M_\epsilon = \begin{bmatrix} A_{01} & B_{01} \\ 0 & 0 \end{bmatrix}, A_{01} = (\delta_{ij}(\delta_i\epsilon))_{n\times n}, B_{01} = (\delta_{ij}(\phi_i\epsilon))_{n\times n}$. It follows that there exists a T such that $S_i(t) > S_i^0 - \epsilon$ for $t > T$; then, $\frac{dI_i}{dt} > \delta_i(S_i^0 - \epsilon)I_i + \phi_i W_i(S_i^0 - \epsilon) - d_v I_i + \sum_{j=1}^n b_{ij} I_j$. Let $v = (v_1, v_2, ..., v_n, v_{n+1}, ..., v_{2n})$ be the positive eigenvector associated with $s(M - M_\epsilon)$, and choose a small enough α to satisfy $(I, W) = (I_1, ..., I_n, W_1, ..., W_n) \geq \alpha v$. By the comparison theorem, $(I, W) \geq \alpha v e^{s(M-M_\epsilon)(t-T)}$, and thus $\lim\limits_{t\to\infty} I_i(t) = \infty, \lim\limits_{t\to\infty} W_i(t) = \infty (i = 1, 2, ..., n)$, a contradiction. Therefore, E^* is the only endemic equilibrium and is globally asymptotically stable.

4. Numerical simulation

Assuming $n = 2$, the effect of sheep immigration on the transmission of brucellosis was studied by numerical simulation. Let $a_{21} = -a_{11}, a_{12} = -a_{22}, b_{21} = -b_{11}, b_{12} = -b_{22}$, and hence, system (2.1) reduces to

$$\begin{cases} \frac{dS_1^h}{dt} = A_1^h - d_{1h}S_1^h - \beta_1 S_1^h I_1 - \alpha_1 S_1^h W_1 + p_1 I_1^h, \\ \frac{dI_1^h}{dt} = \beta_1 S_1^h I_1 + \alpha_1 S_1^h W_1 - d_{1h}S_1^h - p_1 I_1^h - m_1 I_1^h, \\ \frac{dY_1^h}{dt} = m_1 I_1^h - d_{1h} Y_1^h, \\ \frac{dS_1}{dt} = A_1^v - d_{1v}S_1 - \delta_1 S_1 I_1 - \phi_1 W_1 S_1 - a_{21} S_1 + a_{12} S_2, \\ \frac{dI_1}{dt} = \delta_1 S_1 I_1 + \phi_1 W_1 S_1 - d_{1v} I_1 - a_{1v} I_1 - b_{21} I_1 + b_{12} I_2, \\ \frac{dW_1}{dt} = k_1 I_1 - \sigma W_1, \\ \frac{dS_2^h}{dt} = A_2^h - d_{2h}S_2^h - \beta_2 S_2^h I_2 - \alpha_2 S_2^h W_2 + p_2 I_2^h, \\ \frac{dI_2^h}{dt} = \beta_2 S_2^h I_2 + \alpha_2 S_2^h W_2 - d_{2h}S_2^h - p_2 I_2^h - m_2 I_2^h, \\ \frac{dY_2^h}{dt} = m_2 I_2^h - d_{2h} Y_2^h, \\ \frac{dS_2}{dt} = A_2^v - d_{2v}S_2 - \delta_2 S_2 I_2 - \phi_2 W_2 S_2 + a_{21} S_1 - a_{12} S_2, \\ \frac{dI_2}{dt} = \delta_2 S_2 I_2 + \phi_2 W_2 S_2 - d_{2v} I_2 - a_{2v} I_2 + b_{21} I_1 - b_{12} I_2, \\ \frac{dW_2}{dt} = k_2 I_2 - \sigma W_2. \end{cases} \tag{4.1}$$

For system (4.1), the disease-free equilibrium is $P^0 = (S_{1h}^0, 0, 0, S_1^0, 0, 0, S_{2h}^0, 0, 0, S_2^0, 0, 0)$, where $S_{1h}^0 = \frac{A_1^h}{d_{1h}}, S_{2h}^0 = \frac{A_2^h}{d_{2h}}, S_1^0 = \frac{A_1^v a_{12} + A_2^v a_{12} + A_1^v d_{2v}}{a_{12}d_{1v} + a_{21}d_{2v} + d_{1v}d_{2v}}, S_2^0 = \frac{A_1^v a_{21} + A_2^v a_{21} + A_2^v d_{1v}}{a_{12}d_{1v} + a_{21}d_{2v} + d_{1v}d_{2v}}$. Then, the basic reproduction number of the two-patch submodels is calculated as

$R_0 = \frac{1}{2A}(C+D+\frac{\phi_1 S_1^0 B+E}{\sigma})+\frac{1}{2A}\sqrt{(C-D+\frac{\phi_1 S_1^0 B-E}{\sigma})^2+4b_{12}b_{21}\delta_1 S_1^0 \delta_2 S_2^0 - 4b_{12}b_{21}k_2\phi_1 S_1^0 \phi_2 S_2^0}$, where $A = (d_{1v}+a_{1v}+b_{21})(d_{2v}+a_{2v}+b_{12}) - b_{12}b_{21}, B = (d_{2v}+a_{2v}+b_{12})k_1, C = (d_{2v}+a_{2v}+b_{12})\delta_1 S_1^0, D = (d_{1v}+a_{1v}+b_{21})\delta_2 S_2^0, E = (d_{1v}+a_{1v}+b_{21})k_2\phi_2 S_2^0$.

Table 1. Description and parameter values of relevant parameters in the model.

Symbol	Description	Shanxi Province	CI	Hebei Province	CI	Source
A_i^h	The birth number of population in ith patch per unit time	201,164	/	467,718	/	[A]
α_i	Brucella in environment-to-susceptible human transmission rate in ith patch	$1.9e^{-13}$	[$1.9e^{-13}$ $1.9e^{-13}$]	$1.9e^{-13}$	[$1.9e^{-13}$ $1.9e^{-13}$]	fitted
β_i	The infectious sheep-to-susceptible human transmission rate in ith patch	$6.64e^{-09}$	[$6.64e^{-09}$ $6.64e^{-09}$]	$6.64e^{-09}$	[$6.64e^{-09}$ $6.64e^{-09}$]	fitted
d_{ih}	Natural mortality of humans in ith patch	0.0056	/	0.0065	/	[A]
p_i	The acute infected-to-susceptible human transfer rate in ith patch	0.4	/	0.4	/	[24]
m_i	The acute infected-to-chronic infected transfer rate in ith patch	0.6	/	0.6	/	[24]
A_i^v	The birth number of sheep in ith patch per unit time	4,464,653	/	20,346,171	/	[B]
d_{iv}	The sale rate of sheep in ith patch per unit time	0.51	/	1.44	/	[B]
δ_i	The infectious sheep-to-susceptible sheep transmission rate in ith patch	$5.64e^{-08}$	[$2.531e^{-08}$ $8.749e^{-08}$]	$5.648e^{-08}$	[$1.576e^{-08}$ $9.72e^{-08}$]	fitted
ϕ_i	Brucella in environment-to-susceptible sheep transmission rate in ith patch	$1e^{-08}$	[$0.18e^{-08}$ $2.007e^{-08}$]	$3e^{-09}$	[$3.034e^{-09}$ $3.188e^{-09}$]	fitted
a_{iv}	Disease-related culling rate of infectious sheep in ith patch	0.15	/	0.15	/	assumed
a_{ij} $(i \neq j)$	The immigration rate of the susceptible sheep from jth patch to ith patch	$a_{21} = 0.22$	/	$a_{12} = 0.07$	/	assumed
b_{ij} $(i \neq j)$	The immigration rate of the infectious sheep from jth to ith patch	$b_{21} = 0.22$	/	$b_{12} = 0.07$	/	assumed
$-a_{ii}$	The emigration rate of the susceptible sheep in ith patch	$-a_{11} = 0.22$	/	$-a_{22} = 0.07$	/	assumed
$-b_{ii}$	The emigration rate of the infectious sheep in ith patch	$-b_{11} = 0.22$	/	$-b_{22} = 0.07$	/	assumed
k_i	Brucella quantity released by infected sheep in ith patch	0.0056	/	0.0056	/	assumed
σ	Brucella decay rate	0.47	/	0.47	/	assumed

(A) According to The China Statistical Yearbook, $A_{1h} = 201,164, d_{1h} = 0.0056, A_{2h} = 467,718, d_{2h} = 0.0065$.

(B) According to The China Animal Husbandry Statistical Yearbook, in the past eight years, the average stock in Shanxi Province was $8,754,222$, the average sale rate was $d_{1v} = 0.51$, and the birth

number of sheep per unit time was $A_{1v} = 8,754,222 \times 0.51 = 4,464,653$. The average stock in Hebei Province was 14,129,285, the average sale rate was $d_{2v} = 1.44$, and the birth number of sheep per unit time was $A_{2v} = 14,129,285 \times 1.44 = 20,346,171$.

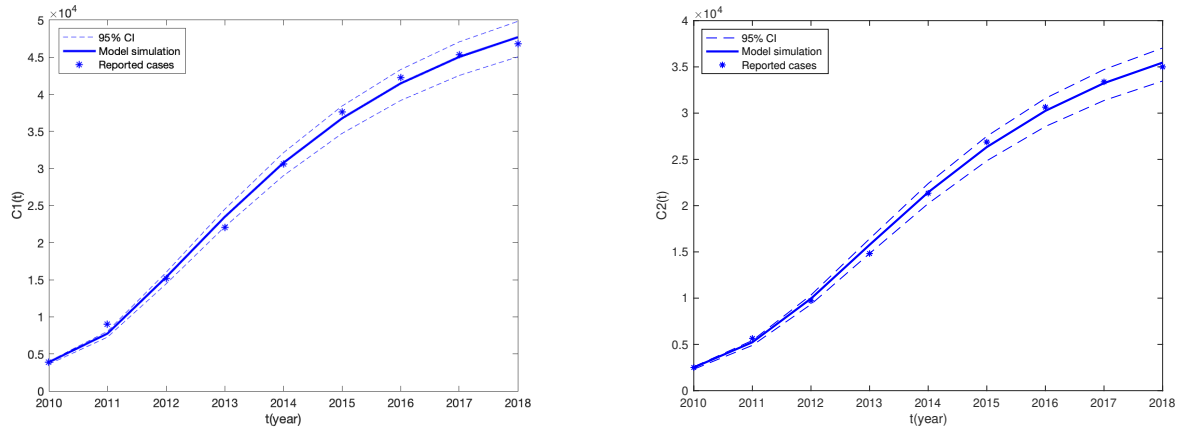

(a) **(b)**

Figure 2. Numerical simulation of the cumulative number of human brucellosis cases in Shanxi and Hebei from 2010 to 2018. The solid line represents the simulation results, these points representing the cumulative reported number of human brucellosis cases from 2010 to 2018, and the dotted line represents the 95% confidence interval. The parameter values are from Table 1. For the initial values, $S_1^{h0} = 35,740,000$, $I_1^{h0} = 3888$, $Y_1^{h0} = 2000$, $S_1^0 = 7,347,000$, $I_1^0 = 1235$, $W_1^0 = 784,670$, $S_2^{h0} = 71,940,000$, $I_2^{h0} = 2503$, $Y_2^{h0} = 1000$, $S_2^0 = 14,086,000$, $I_2^0 = 2142$, $W_2^0 = 220,750$.

4.1. Parameter estimation

Shanxi and Hebei provinces are adjacent provinces with high incidence rates and similar time series. We have chosen the two provinces as the two patches in model (4.1). The rationality of the model is verified by the least squares method using MATLAB. C1 (t) and C2 (t) are defined as the theoretical cumulative numbers of Shanxi Province and Hebei Province in the t year, that is, the solutions of models $\frac{dC1}{dt} = \beta_1 S_1^h I_1 + \alpha_1 S_1^h W_1$ and $\frac{dC2}{dt} = \beta_2 S_2^h I_2 + \alpha_2 S_2^h W_2$. By fitting the model solution with the cumulative number of human brucellosis reported from 2010 to 2018, the values of parameters α_1, α_2, β_1, β_2, δ_1, δ_2, ϕ_1 and ϕ_2 are estimated to obtain $\alpha_1 = \alpha_2 = 1.9e^{-13}$, $\beta_1 = \beta_2 = 6.64e^{-09}$, $\delta_1 = 5.64e^{-08}$, $\delta_2 = 5.648e^{-08}$, $\phi_1 = 1e^{-08}$ and $\phi_2 = 3e^{-09}$. The data used to simulate the model are from article [4], and the model parameter values are from Table 1. Figure 2(a),(b) shows the numerical simulation and 95% confidence interval of the cumulative number of human brucellosis cases in Shanxi and Hebei provinces from 2010 to 2018, respectively. As can be seen from Figure 2, the solution of the model is consistent with the reported data. In addition, we assumed that the number of newly infected people in the two regions obeys the Poisson distribution at time t, and the cumulative cases are C1 (t) and C2 (t), t = 2010,...,2018. If 1000 samples are taken from the Poisson distribution, we have 1000 groups of data samples and make least squares fitting for each group of data. At the same time, 1000 groups of corresponding estimated parameter values can be obtained. We can assume that the parameters obey

the normal distribution, and then we can obtain the 95% confidence interval of the parameters (Table 1). According to the parameter values in the simulation and the basic reproduction number formula in the two patch models, $R_0 = 0.5457$, $R_{01} = 0.7497$, and $R_{02} = 0.5022$, which means that the disease will disappear in Shanxi and Hebei Provinces. This shows that the two regions are very effective in the prevention and control of brucellosis.

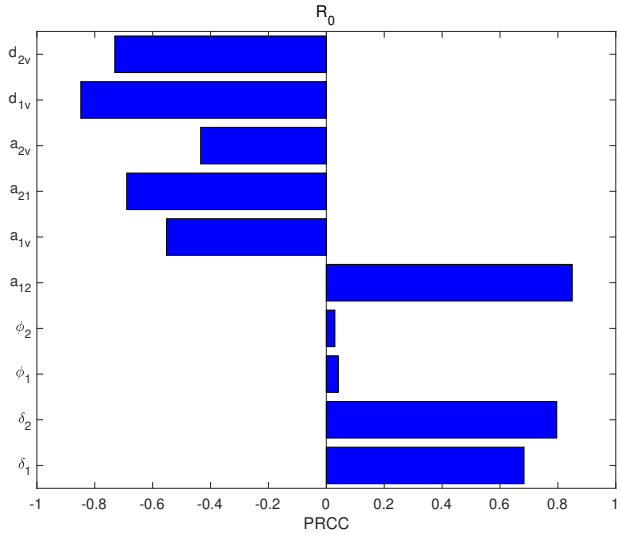

Figure 3. Sensitivity analysis of R_0 using partial rank correlation coefficient (PRCC).

4.2. Sensitivity analysis

As a zoonotic infection, the best way to control human brucellosis is to control the disease in animals. The control measures of livestock brucellosis include detection, vaccination and elimination of infected animals . We should also strengthen information dissemination and health education on brucellosis, and improve veterinary and public health supervision [25]. In this part, we used the PRCC (partial rank correlation coefficient) to analyze the sensitivity of R_0 on control parameters. The control parameters are disease-related culling rates a_{1v} and a_{2v}, the infection rates of infected sheep to susceptible sheep δ_1 and δ_2, infection rates of Brucella to susceptible sheep ϕ_1 and ϕ_2, sheep sales rates d_{1v} and d_{2v}, and sheep immigration rates a_{12} and a_{21}. The sensitivity analysis of basic reproduction number R_0 to parameters is shown in Figure 3. We can observe that R_0 is more sensitive to δ_1, δ_2, a_{12}, a_{1v}, d_{1v} and d_{2v} (|PRCC| > 0.5), in which δ_1, δ_2 and a_{12} are positively correlated (PRCC > 0.5), and a_{1v}, a_{21}, d_{1v} and d_{2v} are negatively correlated (PRCC < -0.5). There may be many factors interacting with human brucellosis. Therefore, when eradicating this disease, we can take a variety of measures, such as timely handling of the infected sheep in the two regions, reducing the infection rate from infected sheep to susceptible sheep in the two regions, decreasing the immigration of sheep from Hebei Province to Shanxi Province and improving the culling rate of infected sheep in Shanxi Province and increasing the sheep immigration rate from Shanxi Province to Hebei Province and the sales rate of sheep in the two regions. The relationships between the basic reproductive number R_0 and the disease-related culling rate a_{2v} of sheep in Hebei Province and the infection rates ϕ_1 and ϕ_2 from Brucella to susceptible sheep of the two regions are weak, so we do not select these three parameters as control parameters. In particular, it can be observed that R_0 has a positive correlation

with the sheep immigration rate (a_{12}) from Hebei Province to Shanxi Province and a negative correlation with the sheep immigration rate (a_{21}) from Shanxi Province to Hebei Province. Therefore, next, we studied the impact of the sheep immigration rate on human brucellosis.

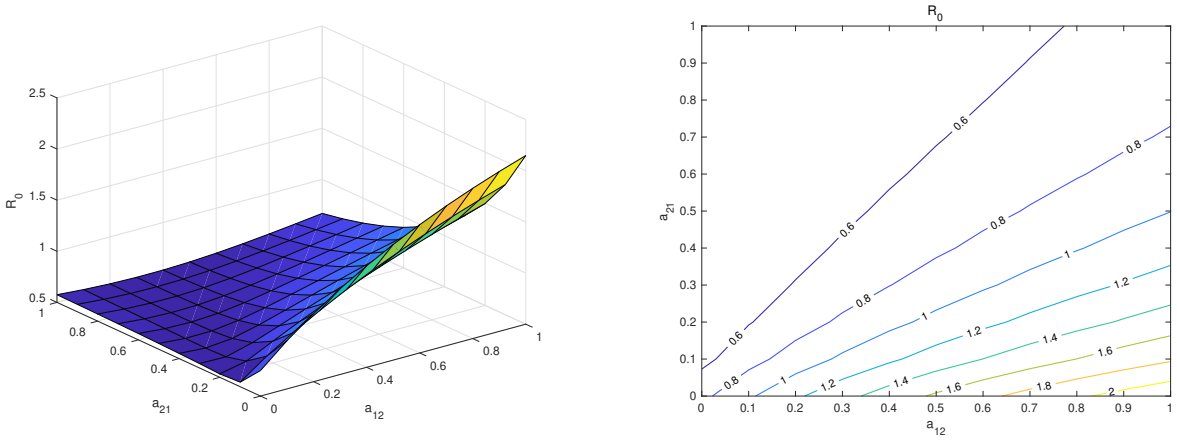

(a) **(b)**

Figure 4. R_0 in terms of parameters a_{12} and a_{21}.

4.3. The influence of sheep immigration on human brucellosis infection

Due to R_0 having the opposite correlation with a_{12} and a_{21}, in this part, we investigated the effects of sheep immigration in Shanxi and Hebei Provinces on human brucellosis infection. Figure 4(a),(b) shows that R_0 is more sensitive to a_{12}. We can reduce the immigration of sheep from Hebei Province to Shanxi Province to control the disease of these two patches. In addition, we chose different immigration rates a_{12} and a_{21} to study the changes of cumulative cases C1, C2 in the two provinces with time t (Figure 5). Figure 5(a) shows that as a_{12} increases, the number of infected cases in the two regions is increasing, and when $a_{12} = 0$, the two regions have the least number of infected individuals. Figure 5(b) shows that as a_{21} increases, the cases in Shanxi Province are decreasing, while the infected in Hebei Province are increasing. When $a_{21} = 0.44$, the least are infected in Shanxi Province, and the most are infected in Hebei Province. When $a_{21} = 0$, the most are infected in Shanxi Province, and the least are infected in Hebei Province. This indicates that in order to have fewer infected, the immigration of sheep cannot be completely absent, the immigration of sheep from Hebei Province to Shanxi Province should be reduced, and the immigration of sheep from Shanxi Province to Hebei Province should be controlled within a reasonable range.

The basic reproduction number R_0 is the expected number of secondary cases produced, in a completely susceptible population, by a typical infective individual [13]. For Shanxi Province and Hebei Province, $R_{01} = 0.7497 > R_{02} = 0.5022$, that is, in the population of all susceptible people, the average number of infected people in Shanxi Province is greater than that in Hebei Province. Here, we refer to Shanxi Province as the high-infected area and Hebei Province as the low-infected area. When there is only one-way immigration ($a_{12} = 0$ or $a_{21} = 0$), the change of cumulative cases C1, C2 with time t in both provinces is shown in Figure 6. When $a_{21} = 0$, only sheep immigrate from the low-infected area to the high-infected area, and Figure 6(a) shows that different values of a_{12} increase

human brucellosis in the high-infected area to different degrees. When $a_{12} = 0$, the increase is minimal. However, the situation of brucellosis in the low-infected zone shown in Figure 6(a) is exactly opposite to that shown in Figure 5(a), where increasing a_{12} will reduce the occurrence of brucellosis in the low-infected zone but increase the occurrence of brucellosis in the high-infected zone. When $a_{12} = 0$ and only sheep immigrate from the high-infected area to the low-infected area, the situation shown in Figure 6(b) is similar to that shown in Figure 5(a) ($a_{12} = 0.07$) for C1, C2 with time t. This indicates that no sheep immigrate from the low-infected area to the high-infected area, or a small amount of immigration has no effect on brucellosis in these two areas. In conclusion, to better reduce human brucellosis in these two areas, there should be some degree of sheep immigration from high- to low-infection areas, and sheep immigration from low- to high-infection areas should be reduced.

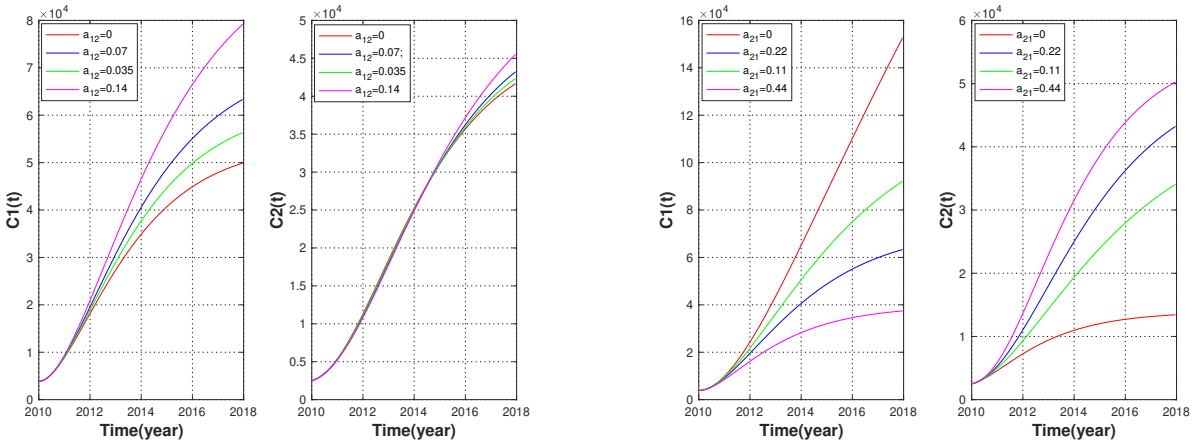

Figure 5. Effects of sheep immigration rates a_{12} and a_{21} on brucellosis in Shanxi and Hebei Provinces.

From the above analysis, it can be seen that in order to better control human brucellosis in the two provinces, there needs to be some sheep immigration between the two provinces. So, what is the amount of sheep immigration under the best condition of disease control? We thought of the case that sheep immigration in these two provinces is a constant C and to minimize R_0 subject to the condition of $a_{21}A_{1v} + a_{12}A_{2v} = C$. We brought $a_{12} = \frac{C - a_{21}A_{1v}}{A_{2v}}$ into the R_0 expression, and then R_0 can be regarded as a function of a_{21}. Different immigration C values were selected to obtain different min R_0. Figure 7 shows that min R_0 first decreases and then increases with the increase of immigration. The maximum immigration under the condition of the best disease control effect is $C = 10,000,000$. The immigration rates of Shanxi Province and Hebei Province are $a_{21} = 0.88$ and $a_{12} = 0.3$, respectively, and the immigration rates are $C_1 = 3,928,894$ and $C_2 = 6,071,105$, respectively.

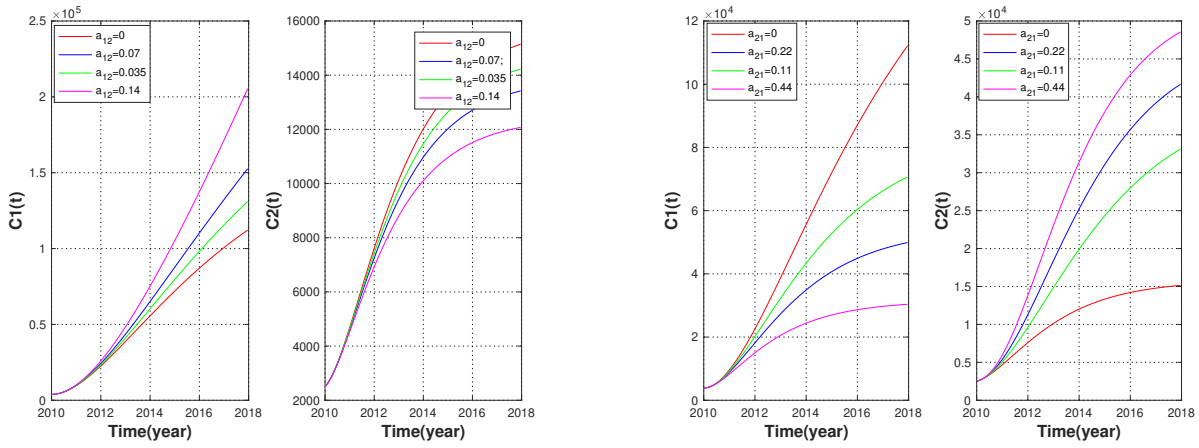

Figure 6. The change of brucellosis between the two areas when sheep immigration occurs in only one area: (a) when there is no sheep immigration from high-infection area to low-infection area (i.e., $a_{21} = 0$), the influence of sheep immigration rate (a_{12}) from low-infection area to high-infection area on the occurrence of brucellosis in these two areas; (b) when there is no sheep immigration from low-infection area to high-infection area (i.e., $a_{12} = 0$), the influence of sheep immigration rate (a_{21}) from high-infection area to low-infection area on the occurrence of brucellosis in these two areas.

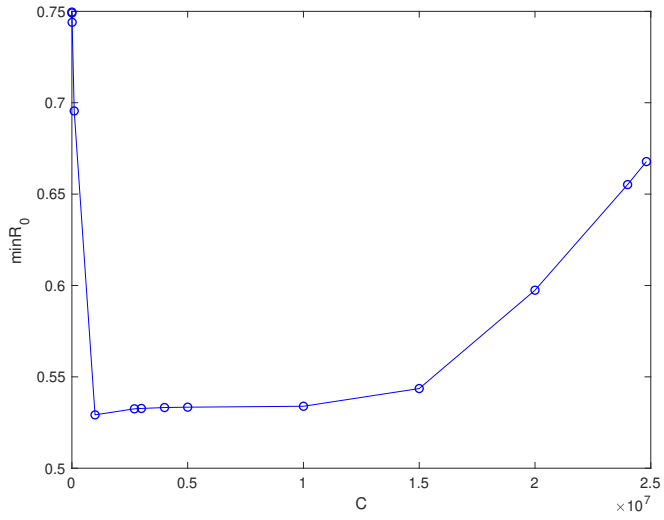

Figure 7. Effects of different sheep immigration value on diseases.

In fact, we collected the data of human brucellosis in Shanxi Province and Hebei Province from 2010 to 2020, and we observed that the number of cases in Shanxi Province and Hebei Province increased sharply in 2019 and 2020. To facilitate our study, we used the number of human brucellosis cases from 2010 to 2018. According to our research, human brucellosis will disappear in the two provinces. Based on the parameters in Table 1, MATLAB was applied to derive the numerical solutions

of cumulative cases C1(t) and C2(t) from 2010 to 2020, and the predicted values of new infections in 2019 and 2020 were obtained according to $I_i^h(t) = Ci(t) - Ci(t-1), i = 1, 2, t = 2019, 2020$. It is predicted that the numbers of human brucellosis cases in Shanxi Province may be 1912 and 1373, and the numbers of human brucellosis cases in Hebei Province may be 1732 and 1258, in 2019 and 2020 (see Figure 8). However, in 2019 and 2020, the actual numbers of cases in Shanxi Province were 3279 and 3365, and in Hebei Province they were 3236 and 2968. There is a huge difference between the predicted data and the actual data. According to our analysis, the main reasons are the occurrence of African swine fever in 2018, the closure of a large number of domestic pig farms and slaughterhouses, a large reduction in the source of pigs, a shortage of pork and a significant increase in prices. Most people chose to buy mutton, and the immigration of sheep in various provinces had also increased greatly, including Shanxi Province and Hebei Province. The frequent trading of sheep products between different regions and the increased mobility of infected animals led to a significant increase in the number of infected people in Shanxi and Hebei provinces in 2019 and 2020, indicating that sheep immigration has a great impact on human brucellosis infection.

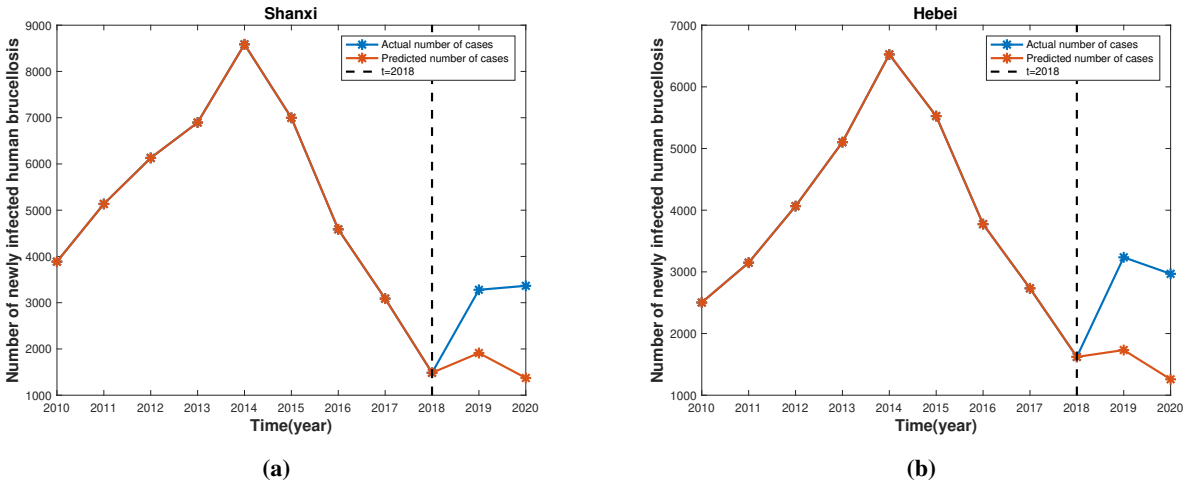

(a) **(b)**

Figure 8. The predicted value and actual value of human brucellosis in Shanxi Province and Hebei Province in 2019 and 2020.

5. Conclusions

In the past 30 years, brucellosis epidemic areas have gradually shifted from pastoral areas to grassland and agricultural areas. Especially since 2004, the affected areas have expanded from the north to the south of China [5, 6], and studies have confirmed that part of the epidemic in the southern region was caused by infected animals imported from other regions [7]. Therefore, the geographical transmission of brucellosis is caused by the immigration of sheep.

In this paper, a patch model was proposed to describe the spatial transmission dynamics of brucellosis and to study the impact of sheep immigration on the geographical transmission of brucellosis. Firstly, we analyzed the dynamics of the model, including the basic reproduction number and the existence, uniqueness and stability of the positive equilibrium.

Secondly, taking Shanxi Province and Hebei Province as examples, numerical simulation was

carried out. The parameters were estimated by the least squares method, and $R_0 = 0.5457$, $R_{01} = 0.7497$ and $R_{02} = 0.0.5022$ were obtained, which indicate that brucellosis will disappear in the two provinces. Sensitivity analysis of R_0 found that the infection rates δ_1 and δ_2 from infected sheep to susceptible sheep, the sheep sale rates d_{1v} and d_{2v}, the sheep immigration rate a_{12} from Hebei Province to Shanxi Province and the disease-related culling rate a_{1v} of sheep in Shanxi Province had greater impacts on R_0. Therefore, when eradicating the disease, we can take a variety of measures, such as vaccinating sheep, timely dealing with infected sheep in these two areas, descreasing the infection rate of infected sheep to susceptible sheep in the two areas, reducing the immigration of sheep from Hebei Province to Shanxi Province, improving the culling rate of infected sheep in Shanxi Province and increasing the sheep immigration rate from Shanxi Province to Hebei Province and the sales rate of sheep in the two regions.

Finally, we studied the influence of sheep immigration rate on the occurrence of disease. In terms of sheep immigration between the two regions, we should minimize the sheep immigration from Hebei Province to Shanxi Province and control the sheep immigration from Shanxi Province to Hebei Province within a reasonable range. According to $R_{01} = 0.7497$ and $R_{02} = 0.5022$, when we only considered one-way immigration, we found that there should be a certain degree of immigration of sheep from high-infection area to low-infection area, and we should lessen the immigration of sheep from low-infection area to high-infection area.

We studied the geographic transmission of sheep brucellosis using a deterministic system and simulated case data from 2010 to 2018 in Shanxi and Hebei provinces. Our model does not consider stochasticity, periodicity and age structure. Next, the patch model combined with these factors can be studied. Meanwhile, only the two-patch model was used to simulate the data of two provinces. Complex transmission among three or more provinces needs to be researched.

Acknowledgments

This work is supported by the National Natural Science Foundation of China under grants (12101443, 11801398) and the Natural Science Foundation of Shanxi Province grants (20210302124260).

Conflict of interest

The authors declare there is no conflict of interest.

References

1. E. J. Richey, C. D. Harrell, Brucella abortus disease (brucellosis) in beef cattle, 1997.
2. M. T. Li, G. Q. Sun, J. Zhang, Z. Jin, X. D. Sun, Y. M. Wang, et al., Transmission dynamics and control for a brucellosis model in Hinggan League of Inner Mongolia, China, *Math. Biosci. Eng.*, **11** (2014), 1115–1137. https://doi.org/10.3934/mbe.2014.11.1115
3. M. N. Seleem, S. M. Boyle, N. Sriranganathan, Brucellosis: A re-emerging zoonosis, *Vet. Microbiol.*, **140** (2009), 392–398. https://doi.org/10.1016/j.vetmic.2009.06.021
4. G. Q. Sun, M. T. Li, J. Zhang, W. Zhang, Z. Jin, Transmission dynamics of brucellosis: Mathematical modelling and applications in China, *Comput. Struct. Biotechnol. J.*, **18** (2020), 3843–3860. https://doi.org/10.1016/j.csbj.2020.11.014
5. Y. Lin, M. H. Xu, X. Y. Zhang, T. Zhang, An exploratory study of factors associated with human brucellosis in mainland China based on time-series-cross-section data from 2005 to 2016, *PLoS ONE*, **14** (2019), e0208292. https://doi.org/10.1371/journal.pone.0208292
6. S. J. Lai, H. Zhou, W. Y. Xiong, M. Gilbert, Z. J. Huang, J. X. Yu, et al., Changing epidemiology of human brucellosis, China, 1955–2014, *Emerg. Infect. Dis.*, **23** (2017), 184. https://doi.org/10.3201/eid2302.151710
7. H. Jiang, M. G. Fan, J. D. Chen, J. C. Mi, B. Y. Cui, MLVA genotyping of Chinese human Brucella melitensisbiovar 1, 2 and 3 isolates, *Bmc. Microbiol.*, **11** (2011), 256–256. https://doi.org/10.1186/1471-2180-11-256
8. X. Ma, X. F. Luo, L. Li, Y. Li, G. Q. Sun, The influence of mask use on the spread of COVID-19 during pandemic in New York City, *Results Phys.*, **34** (2022), 105–224. https://doi.org/10.1016/j.rinp.2022.105224
9. K. K. J. Asamoah, O. Eric, A. Abidemi, S. E. Moore, G. Q. Sun, Z. Jin, et al., Optimal control and comprehensive cost-effectiveness analysis for COVID-19, *Results Phys.*, **33** (2022), 105–117. https://doi.org/10.1016/j.rinp.2022.105177
10. Q. Hou, X. D. Sun, Modeling sheep brucellosis transmission with a multi-stage model in Changling County of Jilin Province, China, *J. Appl. Math. Comput.*, **51** (2016), 227–244. https://doi.org/10.1007/s12190-015-0901-y
11. Q. L. Chen, S. J. Lai, W. W. Yin, H. Zhou, Y. Li, D. Mu, et al., Epidemic characteristics, high-risk townships and space-time clusters of human brucellosis in Shanxi Province of China, 2005–2014, *BMC Infect. Dis.*, **16** (2016), 1–10. https://doi.org/10.1186/s12879-016-2086-x
12. J. Zhang, S. G. Ruan, G. Q. Sun, X. D. Sun, Z. Jin, Analysis of a multi-patch dynamical model about cattle brucellosis, *J. Shanghai Norm. Univ. : Nat. Sci. Math.*, **43** (2014), 15.
13. P. Dreessche, J. Watmough, Reproduction numbers and sub-threshold endemic equilibria for compartmental models of disease transmission, *Math. Biosci.*, **180** (2002), 29–48. https://doi.org/10.1016/S0025-5564(02)00108-6
14. H. Smith, *Monotone Dynamical Systems : An Introduction to the Theory of Competitive and Cooperative Systems*, Ams Ebooks Program, 1995. http://dx.doi.org/10.1090/surv/041

15. M. Y. Li, *An Introduction to Mathematical Modeling of Infectious Diseases*, Cham, Switzerland, 2018. https://doi.org/10.1007/978-3-319-72122-4

16. R. A. Horn, C. R. Johnson, *Topics in Matrix Analysis*, Cambridge University Press, 1985. https://doi.org/10.1017/CBO9780511810817

17. D. Gao, S. Ruan, A multipatch malaria model with logistic growth populations, *SIAM J. Appl. Math.*, **72** (2012), 819–841. https://doi.org/10.1137/110850761

18. J. K. Hale, O. Lopes, Fixed point theorems and dissipative processes, *J. Differ. Equations*, **12** (1973), 391–402. https://doi.org/10.1016/0022-0396(73)90025-9

19. H. K. Khalil, Y. S. Zhu, H. Dong, Z. Z. Li, *Nonlinear Systems*, 3nd edition, Publishing House of Electronics Industry, Bei Jing, 2005.

20. Thieme, R. Horst, Persistence under relaxed point-dissipativity (with application to an endemic model), *Siam J. Math. Anal.*, **24** (2006), 407–435. https://doi.org/10.1137/0524026

21. X. Q. Zhao, Uniform persistence and periodic coexistence states in infinite-dimensional periodic semiflows with applications, *Can. Appl. Math. Q.*, **3** (1995), 473–495.

22. X. Zhao, Z. Jing, Global asymptotic behavior in some cooperative systems of functional differential equations, *Can. Appl. Math. Q.*, **4** (1996), 421–444.

23. X. Q. Zhao, *Dynamical Systems in Population Biology*, Springer, New York, 2003. https://doi.org/10.1007/978-3-319-56433-3

24. Q. Hou, X. D. Sun, J. Zhang, Y. J. Liu, Z. Jin, Modeling the transmission dynamics of sheep brucellosis in Inner Mongolia Autonomous Region, China, *Math. Biosci.*, **242** (2013), 51–58. https://doi.org/10.1016/j.mbs.2012.11.012

25. H. Jiang, D. O'Callaghan, J. B. Ding, Brucellosis in China: History, progress and challenge, *Infect. Dis. Poverty*, **9** (2020). https://doi.org/10.1186/s40249-020-00673-8

AIMS Press